Chinese Journal of Catalysis 71 (2025) 169–178

available at www.sciencedirect.com

ScienceDirect

journal homepage: www.sciencedirect.com/journal/chinese-journal-of-catalysis

Article

The role of C1 species in the methanol-to-hydrocarbons reaction: Beyond merely being reactants

Yanan Zhang [a,c], Wenna Zhang [a,*], Chengwei Zhang [a,c], Linhai He [a,c], Shanfan Lin [a], Shutao Xu [a], Yingxu Wei [a,*], Zhongmin Liu [a,b,c]

[a] *National Engineering Research Center of Lower-Carbon Catalysis Technology, Dalian National Laboratory for Clean Energy, iChEM (Collaborative Innovation Center of Chemistry for Energy Materials), Dalian Institute of Chemical Physics, Chinese Academy of Sciences, Dalian 116023, Liaoning, China*

[b] *State Key Laboratory of Catalysis, Dalian Institute of Chemical Physics, Chinese Academy of Sciences, Dalian 116023, Liaoning, China*

[c] *University of Chinese Academy of Sciences, Beijing 100049, China*

ARTICLE INFO

Article history:
Received 05 November 2024
Accepted 18 December 2024
Available online 20 April 2025

Keywords:
Methanol-to-hydrocarbons
C1 species
Methylation
Hydride-transfer
Confined zeolite microenvironments
SAPO-34

ABSTRACT

In the methanol-to-hydrocarbons (MTH) process, C1 species, including methanol, dimethyl ether, and surface methoxy species (SMS), play crucial roles in the evolution of organic species and the construction of reaction networks. Understanding the roles of C1 species throughout the entire MTH process is both essential and challenging. Herein, the dynamic evolution of organic species and unique variation of C1 species during the real-time MTH process were observed by *operando* diffused reflectance Fourier transform infrared spectroscopy and *ex-situ* ^{13}C cross polarization/magic-angle spinning nuclear magnetic resonance experiments. Importantly, density functional theory calculations thoroughly illustrated that methanol and SMS serve as key C1 species, in the form of not only methylation agents but also hydride acceptors, and their contributions vary across different reaction periods. Initially, SMS acts as the preferential C1 surface intermediate, methylating with hydrocarbons to propagate C–C bond, while also accepting hydrides to generate precursors for active hydrocarbon pool species. As reaction progresses, the role of SMS gradually diminishes, and thereby methanol becomes the predominant C1 species, in methylation for efficient product formation, meanwhile in hydride-transfer causing catalyst deactivation. Additionally, it was demonstrated that the confined zeolite microenvironment modified by large organics affects methanol adsorption and SMS formation, also accounting for the absence of SMS during the later period of reaction. This work provides a comprehensive and systematic understanding of the dynamic roles of C1 species throughout the MTH process, beyond the role as reactants.

1. Introduction

Methanol-to-hydrocarbons (MTH), a pivotal reaction in C1 chemistry, provides a diverse product distribution including light olefins, aromatics, and gasoline *via* the non-oil route from abundant coal, natural gas, or biomass resources [1]. With decades of research and progressive understanding, the dynamic catalytic mechanisms of MTH reaction have been revealed [2–5]. The dynamic MTH reaction process starts with the initial methanol dehydration catalyzed by Brønsted acid

* Corresponding author. E-mail: zhangwn@dicp.ac.cn (W. Zhang), weiyx@dicp.ac.cn (Y. Wei).

This work was supported by the National Key R&D Program of China (2021YFA1502600), the National Natural Science Foundation of China (22372169, 22002157, 22402190, 21991092, 21991090, 22288101), and the Liaoning Provincial Natural Science Foundation of China (2022-BS-019).
https://doi.org/10.1016/S1872-2067(24)60228-7

sites (BAS), and subsequently turns into an organic-inorganic hybrid supramolecular system-mediated autocatalysis process that can be divided into three reaction periods: the induction stage, highly efficient stage, and deactivation stage. C1 species, encompassing methanol, dimethyl ether (DME), and surface methoxy species (SMS), correlate closely with the evolution of organic species and the construction of complex reaction networks in methanol conversion process. In our previous works [2,4–6], the *operando* diffused reflectance Fourier transform infrared spectroscopy (DRIFTS) with online mass spectroscopy were utilized to monitor the dynamic evolution of catalyst surface species and effluent species during methanol conversion. It is noteworthy that C1 species not only work as reactants for MTH reactions, but also provide "fuel" for powering the autocatalytic system and dominating the autocatalysis by collaborating with active hydrocarbon pool (HCP) species, as shown in Scheme 1. However, in the course of reaction, the specific roles of various C1 species, including methanol, DME, and SMS, in their interactions with HCP species and inactive polyaromatic compounds remain unclear in this complicated MTH reaction system.

For the MTH reaction system, multiple elementary reactions such as methylation, cyclization, hydride transfer, and cracking/dealkylation construct the complex reaction network of methanol conversion [7,8]. Thereinto, C1 species can serve as methylation agents in methylation reactions to realize the carbon chain growth of hydrocarbon molecules, and simultaneously, they can act as hydride acceptors in hydride-transfer reactions to generate highly unsaturated active cyclic species (cyclopentenyl/phenyl species) or inactive polycyclic aromatic hydrocarbons (PAHs). Numerous experiments and theoretical calculations have been carried out to investigate the role of C1 species in methylation and hydride-transfer reactions in MTH process with specific organic species present in zeolite catalyst [8–12]. The methylation of alkenes with methanol over ZSM-22 zeolite demonstrated that SMS-involved stepwise methylation route prevails at conditions of temperature above 600 K and total pressure below 1 bar, while the MeOH-involved concerted methylation pathway can occur at lower temperatures and/or higher pressures [9]. In the methylation of polymethylbenzenes with methanol and DME, density functional theory (DFT) calculations suggested that both sequential and concerted methylation mechanisms can occur, and these two C1 species are equally capable of converting methylbenzene species [10]. In hydride-transfer reactions, methoxy is generally chosen as the representative hydride acceptor for transferring hydrogen atoms from cycloalkanes, cycloalkenes, and cyclodienes to generate aromatics or aging of naphthalene species into larger polycyclic aromatics to cause catalyst deactivation [11,12]. Additionally, the reaction of isobutene with methanol or DME over ZSM-5 zeolite revealed that methanol can react with isobutene through hydride transfer, competing with methylation, while the reaction of DME with isobutene is substantially dominated by the route of methylation [8]. These reports clarified the vital role of different C1 species interacting with several organic species via methylation and hydride-transfer reactions. However, with the MTH reaction proceeding, a comprehensive and systematic understanding of the role of different C1 species, varied by the zeolite microenvironment with the modification of confined organic species, has not yet been developed.

In this work, the *operando* DRIFTS and *ex-situ* ^{13}C cross polarization/magic-angle spinning nuclear magnetic resonance (CP/MAS NMR) experiments were performed to track the dynamic evolution of C1 species and retained organic species over SAPO-34 under the real-time MTH reaction process. Particularly, it is noticeable that the signals of different C1 species evolved with the reaction progress. Furthermore, DFT calculations were adopted to explore the role of C1 species (methanol and SMS) in the whole MTH process via evaluating methylation and hydride-transfer reactions with representative hydrocarbon species theoretically. In addition, given the absence of SMS at the later period of reaction, the influence of zeolite microenvironment with the involvement of large organic species on methanol adsorption and SMS formation were further elucidated at the microscale to reveal the role of specific zeolite environment.

2. Experimental

2.1. Catalyst preparation

The SAPO-34 sample used in this work was synthesized fol-

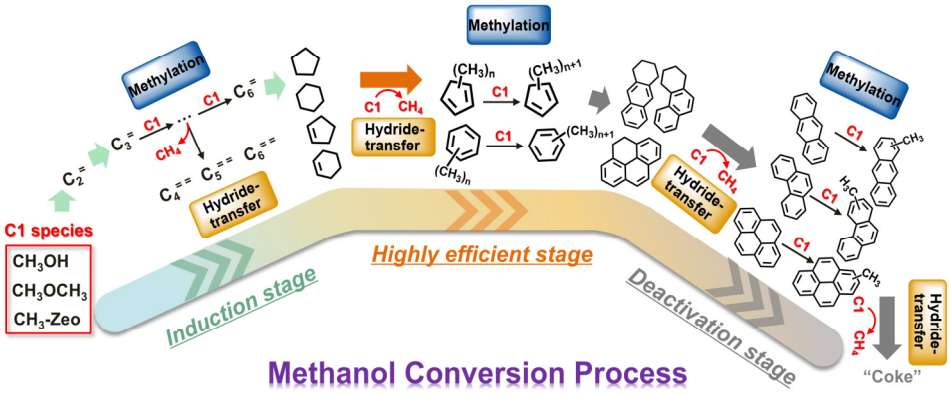

Scheme 1. Dynamic catalytic process of MTH reaction with C1 species participation.

lowing the procedure described in our previous work [13]. The fresh H-form SAPO-34 was obtained by calcining the crystallized products at 873 K in 100 mL min^{-1} air flow for 6 h to remove organic templates.

2.2. Catalyst characterizations

The characterization results of powder X-ray diffraction (XRD), scanning electron microscopy (SEM), and X-ray fluorescence (XRF) are detailed in Figs. S1, S2 in the Supporting Information (SI).

2.3. Catalytic tests

Methanol conversion experiments were carried out in a fixed-bed quartz tube reactor with an inner diameter of 4 mm under atmospheric pressure. The catalyst powder was pressed and sieved into 40–60 mesh. 100 mg of 40–60 mesh catalyst was firstly packed into the reactor and activated under nitrogen flow at 723 K for 30 min, and then the temperature was decreased to reaction temperature (623 K). The methanol was fed by passing nitrogen through a saturation evaporator kept at 288 K with a weight hourly space velocity (WHSV) of 2 h^{-1}. The effluents were analyzed by an online gas chromatograph (GC, Agilent 7890B) equipped with a PoraPLOT Q capillary column and a flame ionization detector. The methanol conversion and product selectivity of reaction were calculated on a CH_2 basis, as both methanol and dimethyl ether were considered as reactants in the calculation.

2.4. Operando DRIFTS experiments

The *Operando* DRIFTS experiments were performed on a Bruker Tensor 27 instrument equipped with a diffuse reflectance infrared cell with ZnSe window and a liquid nitrogen-cooled Hg-Cd-Te detector. 20–30 mg catalyst powder was loaded in the reaction cell and activated under nitrogen flow at 723 K for 30 min, and then the temperature was decreased to reaction temperature. The methanol was fed by passing 25 mL min^{-1} nitrogen through a saturation evaporator kept at 288 K. Once methanol was continuously introduced into the reaction cell loaded with catalyst, the DRIFT spectra were collected instantly by averaging 16 scans at 4 cm^{-1} resolution.

2.5. $^{12}C/^{13}C$-methanol switch experiments

The $^{12}C/^{13}C$-methanol switch experiments were conducted at 623 K over SAPO-34, and methanol was fed in following the procedures described in catalytic testing. The ^{12}C-methanol was firstly fed for a series of reaction time to build up the hydrocarbon pool with confined ^{12}C-organic species, and then ^{13}C-methanol was switched into the reactor for 30 sec to obtain ^{13}C-labelled organic species retained in catalyst samples. Subsequently, the reactant flow was cut off and the reactor was cooled immediately by liquid nitrogen. The organic species retained in catalysts were analyzed by solid-state NMR spectroscopy.

2.6. ^{13}C CP/MAS NMR measurements

After $^{12}C/^{13}C$-methanol switch experiments, the reaction tube was sealed by two globe valves and transferred to the glove box to load catalyst samples into an NMR rotor. The ^{13}C CP/MAS NMR spectra were collected on a Bruker Avance NEO 500 MHz spectrometer equipped with a 11.7 T and 89 mm wide-bore magnet using a 3.2 mm H/F-X-Y triple resonance MAS probe with the corresponding Larmor frequencies of 125.765 and 500.13 MHz for the ^{13}C and ^{1}H nucleuses, respectively. The 1D ^{1}H-^{13}C cross-polarization (CP) spectra were recorded with a spinning rate of 12 kHz. 2048 scans were accumulated with a π/2 pulse length of 3.6 μs for ^{1}H, a cross-polarization contact time of 3.0 ms, and a recycle delay of 2 *s*. The decoupling field of 69.45 kHz was applied during the acquisition time. The ^{13}C chemical shifts are referenced to adamantane with the up-field methine peak at 29.5 ppm.

2.7. Theoretical calculation model and method

The CHA structure (cell parameters: $a = b = 13.6750$ Å, $c = 14.7670$ Å, $\alpha = \beta = 90°$, $\gamma = 120°$) was obtained from the International Zeolite Association (IZA) database. For theoretical calculations, H-SAPO-34 was represented by an extended 84T ($Si_1P_{41}Al_{42}O_{139}H_{57}$) cluster model (Fig. S4) extracted from the crystallographic CHA structure. The terminal T–O bonds were saturated by hydrogen atoms, oriented along the direction of the corresponding T–O bond. Atoms in line were set to the low layer, and atoms in ball were set to the high layer. The location of Brønsted acid site was chosen at O3 site (one 4-MR, 6-MR, and 8-MR) in the 8-MR pore opening.

The ONIOM method [14] was employed to optimize the geometries of reactant adsorption and transition states. The method ωB97XD/6-311G(d,p):AM1 was applied to optimize geometries of high-level and low-level layers, where the active center with its surrounding shells was in the high-level layer while the rest was in the low-level layer. To preserve original zeolite structure and accurate simulation, only terminal hydrogen atoms were fixed at crystallographic locations and other atoms were relaxed. The frequency calculation was performed at the same level as geometry optimization to ensure the saddle points exhibit a proper number of imaginary frequencies. The single-point energy was calculated at the ωB97XD/6-311G(2df,2p) method and corrected by zero-point vibration energy to obtain highly accurate energy. In order to be consistent with the real MTH reaction condition, the Gibbs free energy was calculated by the total electronic energy and thermal correction from frequency calculation. All DFT calculations were performed with the Gaussian 09 package [15].

When large organic species are confined in zeolite microenvironment, the Gibbs adsorption energy of methanol is defined as follows:

$$\Delta G_{MeOH} = G_{(Zeolite–MeOH\&Organics)} - G_{(Zeolite–Organics)} - G_{MeOH(g)}$$

herein, $G_{(Zeolite–MeOH\&Organics)}$, $G_{(Zeolite–Organics)}$, and $G_{MeOH(g)}$ represent the Gibbs energy of the system with interaction between methanol and organic species, the Gibbs energy of adsorbed organic species, and the Gibbs energy of methanol in gas phase,

respectively.

3. Results and discussion

3.1. Dynamic evolution of organic species and unique variation of C1 species during the real-time MTH process

The dynamic evolution of C1 species and retained organic species over SAPO-34 was tracked by *operando* DRIFTS experiments during continuous flow conversion of methanol at 623 K, as shown in Fig. 1(a). With the feeding of methanol, the BAS signal [16] at 3610 and 3590 cm^{-1} gradually weakened, while simultaneously, adsorbed methanol (2956 and 2852 cm^{-1}) [17,18] underwent instantaneous dehydration, leading to the formation of DME (3010, 2945, and 2840 cm^{-1}) [17,18] and SMS (2977, 2867 cm^{-1} from the stretching vibration of C–H bond, and 938 cm^{-1} from the stretching vibration of C–O bond) [17–19]. Remarkably, the intensity of SMS increased significantly for a brief period of time, then decreased until it completely disappeared as the reaction proceeded. Concurrently, cyclopentenyl and phenyl species (1510, 1600 cm^{-1}) [20,21] appeared and gradually increased in intensity. Additional *operando* DRIFTS experiments of methanol conversion at 573, 548, and 473 K were also performed, and the corresponding spectra are shown in Fig. S3. As the reaction temperature decreased, the signal of SMS changed similarly, but with a prolonged signal duration until decay or disappearance. The aforementioned *operando* DRIFTS experimental findings revealed the dynamic evolution of C1 species and retained organic species over SAPO-34 under the real-time MTH reaction process. Importantly, the uncovered unique patterns of SMS variation as methanol conversion progresses imply the diverse functional contributions of C1 species with the formation and evolution of reaction intermediates throughout the MTH process.

In order to thoroughly analyze C1 species on the SAPO-34 surface and their conversion by the interaction with the retained organics in catalysts during the methanol conversion process, *ex-situ* ^{13}C CP/MAS NMR measurements were conducted after $^{12}C/^{13}C$ methanol switch experiments. Based on methanol conversion versus time on stream over SAPO-34 at 623 K (Fig. 1(b)), ^{12}C-methanol was firstly fed into a fixed-bed reactor for 2, 25, 50, 70, and 100 min, respectively, to build up the ^{12}C-hydrocarbon pool, followed by the conversion of ^{13}C-methanol for 30 s to obtain ^{13}C-labelled organic species with different reaction time. Subsequently, the *ex-situ* ^{13}C CP/MAS NMR spectra were recorded to detect the C1 species and retained organic species over SAPO-34. In Fig. 1(c), the signals of aromatics (130 and 135 ppm) [22] were obviously observed. Besides the presence of these neutral organic species, cyclopentenyl carbocations (153 and 245 ppm) [23] and aromatic carbocations (141, 189 and 198 ppm) [24] also appeared in the catalyst sample at 2 min. The signals of C1 species, such as adsorbed methanol (47, 51, and 53 ppm) [25,26], SMS (56.5 ppm) [25,26] and DME (61 and 63 ppm) [25,26], were evidently captured in the catalyst sample at 2 min. This means the possibility of C1 species participation in MTH at this moment in the form of adsorbed methanol, DME, and intermediate of SMS. With the progression of reaction, these signals of C1 species over SAPO-34 gradually weakened at 25, 50, and 70 min, indicating the significant consumption of these C1 reactants and intermediate species. During the deactivation period,

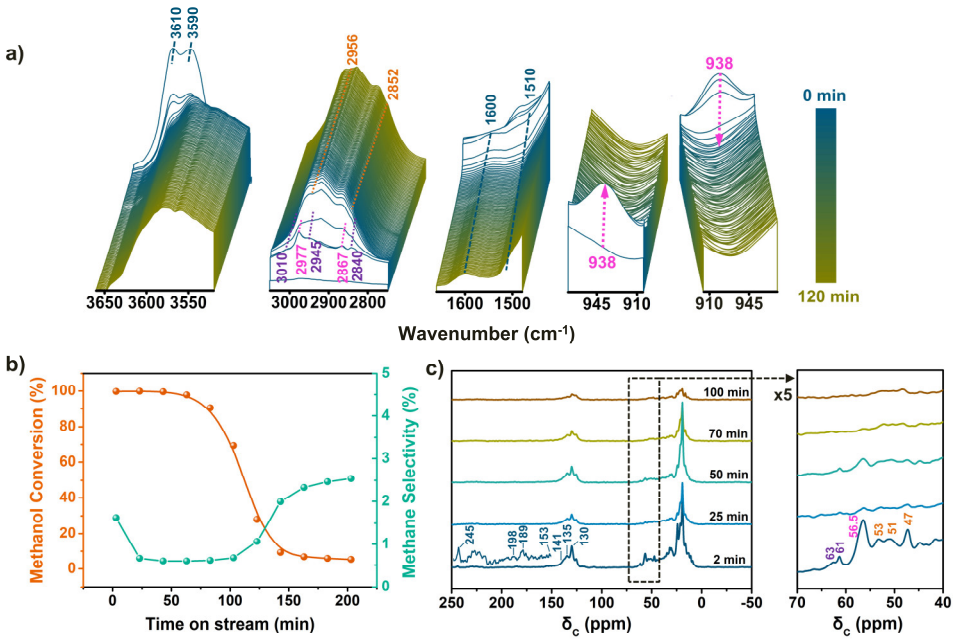

Fig. 1. (a) *Operando* DRIFT spectra for continuous flow conversion of methanol over SAPO-34 at 623 K. (b) Methanol conversion and methane selectivity versus time on stream for methanol conversion over SAPO-34 at 623 K. (c) ^{13}C CP/MAS NMR spectra of SAPO-34 with retained organics recorded after $^{12}C/^{13}C$-methanol switch experiments (^{12}C-methanol feeding for 2, 25, 50, 70, and 100 min followed by ^{13}C-methanol feeding for 30 sec) over SAPO-34 at 623 K. The signals of adsorbed methanol, SMS, and adsorbed DME are labelled in orange, pink, and purple colors, respectively.

the signals of DME and SMS were absent, while the signal of methanol at 47 ppm was still detectable at 100 min. These variations of different C1 species signals during different reaction time imply that their transformation and interaction with retained organic species vary across reaction stages. During the period of efficient methanol conversion before 70 min, the presence of C1 species (methanol, DME, and SMS) indicates that they can contribute to C–C bond propagation *via* methylation reactions, thereby facilitating efficient product formation. With the deactivation of catalyst after 70 min, large confined organic species can block the pore openings and zeolite cavities, occupy BAS, and thus inhibit the diffusion of C1 reactants and the generation of SMS. This result corresponds to the weakened signal of methanol and the disappearance of SMS in the spectra at 100 min.

Moreover, regarding the selectivity of methane in the fixed-bed methanol conversion process (Fig. 1(b)), methane, as a C1 by-product, was formed in the initial and deactivation stages. The formation of methane in the initial stage can be attributed to the hydride-transfer reaction between SMS and methanol [27] and the secondary hydride-transfer reactions between methanol and hydrocarbon products or retained cyclic organics can account for the generation of methane during the deactivation stage [28]. Associated with the variations of C1 species signals during the methanol conversion process shown in the *ex-situ* ^{13}C CP/MAS NMR spectra, methane may originate from different C1 species via hydride-transfer reactions at the initial stage and deactivation stage. These experimental results highlighted the unique variation of C1 species signals along with reaction time and revealed the different involvement of C1 species in the dynamic methanol conversion process, especially for methanol and SMS. This motivates a detailed exploration of the roles of C1 species throughout the entire MTH reaction process.

3.2. Prevailing reaction pathways with C1 species involved and their contributions throughout the entire MTH process

Methanol as a C1 reactant and SMS as a C1 surface intermediate can both serve as methylation agents or hydride acceptors by interacting with retained organic species in the MTH reaction process. As elaborated in Fig. 2(a), SMS can be initially generated from adsorbed methanol with the release of a water molecule [29–31]. Subsequently, SMS interacts with hydrocarbon species through two reaction routes: methylation reaction, where it acts as a methylation agent to extend the C–C bond, and hydride-transfer reaction, where it serves as a hydride acceptor to enhance the unsaturation of the precursors for the formation of active HCP species or PAHs. Concurrently, methanol can react directly with these hydrocarbon species via competing reaction routes, producing methylated or highly unsaturated products with the release of a water molecule [25,32–34]. For the different involvement of SMS and methanol during the whole MTH reaction, the dominant C1 species at different reaction stages and their distinct roles remain inadequately understood and require thorough investigation. To address this, DFT calculations were performed to compare the SMS/MeOH-involved methylation and hydride-transfer reactions with representative hydrocarbon species across different reaction periods, elucidating the prevailing reaction pathways and clarifying the contributions of different C1 species throughout the entire MTH process. The representative hydrocarbon species consist of C_2–C_4 alkenes, C_4–C_6 dienes, C_5–C_6 cycloalkanes, cycloalkenes, cyclodienes and benzene, polymethyl-cyclopentadiene/benzene, naphthyl species, 2H/4H-PAHs, and PAHs.

In SMS-Zeolite/$MeOH_{ads}$-Zeolite hybrid supramolecular catalytic systems, SMS or MeOH-involved methylation and hydride-transfer reactions with representative hydrocarbon species at different reaction periods were calculated, and the Gibbs free energy profile is shown in Fig. 2(b). In methylation reactions of alkenes (from ethene to butene), the free energy barriers for SMS-involved reaction pathways (117.8–139.9 kJ/mol) were lower than those for MeOH-involved reaction pathways (127.2–147.1 kJ/mol), indicating that SMS is slightly superior to methanol in methylation with C_2–C_4 alkenes. When methylating highly unsaturated dienes, the free energy barriers for SMS-involved (125.0–161.5 kJ/mol) and MeOH-involved (130.9–167.5 kJ/mol) reaction pathways were close, suggesting an almost equal contribution of methanol and SMS to the methylation of dienes. In MTH reaction, cyclic species, generated from long-chain alkenes and dienes through cyclization and hydride-transfer reactions, react with methylation agents to produce active HCP species. In the methylation of C_5–C_6 cycloalkenes, cyclodienes, and benzene, the free energy barriers for SMS-involved methylation routes (81.5–143.7 kJ/mol) were lower than those for MeOH-involved methylation routes (124.9–165.8 kJ/mol) by 12–43 kJ/mol, suggesting that the reactivity of SMS in the methylation of cycloalkenes, cyclodienes, and benzene is relatively stronger than that of methanol. Surprisingly, for the MTH reaction at the highly efficient period, it was found that the dominant reaction pathway undergoes a gradual transition towards the MeOH-involved route with the increase of methyl groups in active HCP species. In Fig. S5, the free energy barriers for SMS-involved methylation of mono/di-methylcyclopentadiene (124.7/94.2 kJ/mol) and mono/di-methylbenzene (135.0/119.9 kJ/mol) were lower than those for MeOH-involved methylation (129.5/99.0, 163.3/149.2 kJ/mol). However, these two reaction pathways presented little difference in the methylation of trimethylcyclopentadiene and trimethylbenzene, with very close free energy barriers (97.9 *vs.* 95.7 kJ/mol, 133.3 *vs.* 131.2 kJ/mol). As the free energy barriers for SMS-involved methylation increased significantly, the MeOH-involved reaction route became the prevailing pathway for the methylation of tetramethylcyclopentadiene (109.1 *vs.* 133.8 kJ/mol) and tetra/penta-methylbenzene (123.6/113.4 *vs.* 148.2/136.0 kJ/mol). Moreover, methylation of more active HCP species with methanol, including pentamethylcyclopentadiene (PMCP, 101.5 *vs.* 124.5 kJ/mol), hexamethylbenzene (HMB, 108.9 *vs.* 134.3 kJ/mol), and dimethylnaphthalene (DMN, 124.6 *vs.* 126.9 kJ/mol), also exhibited lower free energy barriers than SMS-involved reaction pathways. Thus, it suggests that with the increase of methyl substitutions, active HCP species are more

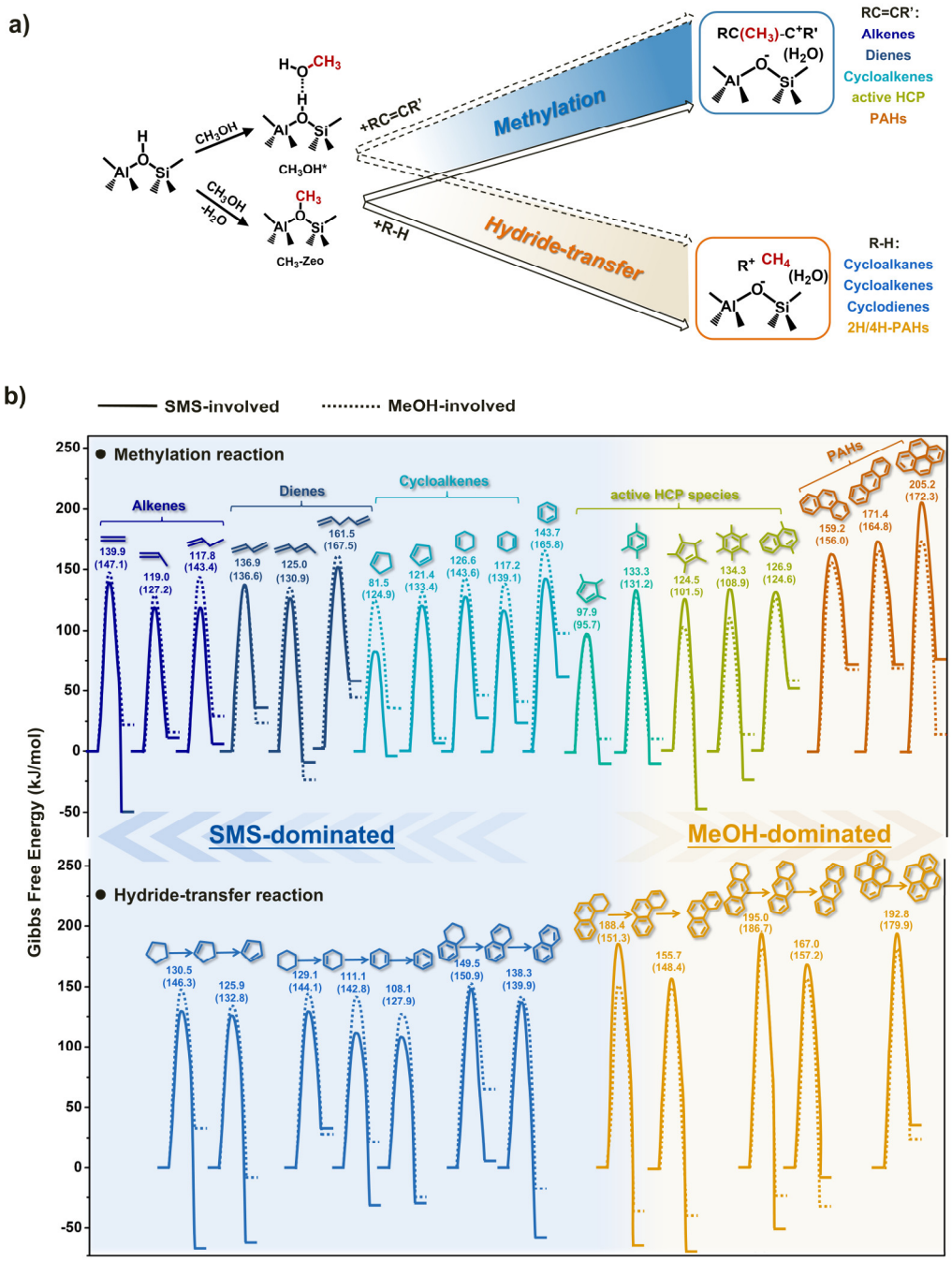

Fig. 2. (a) The schematic diagram of methylation and hydride-transfer reaction routes of SMS/MeOH with representative organic species. (b) The Gibbs free energy profile of methylation and hydride-transfer reactions with SMS (solid line) and MeOH (dash line) participation at 673 K.

inclined to be methylated with methanol, promoting the efficient participation of methanol feeding. For the MTH reaction during catalyst deactivation, PAHs occur as coke precursors via cyclization and continuous hydride-transfer reactions from active HCP species. The free energy barriers for SMS-involved and MeOH-involved methylation reactions of PAHs were significantly high (159.2–205.2 and 156.0–172.3 kJ/mol, respectively), but it is noteworthy that the free energy barriers for the MeOH-involved methylation reaction route were lower than those for the SMS-involved methylation reaction pathway, indicating that the MeOH-involved reaction route continues to work as the dominant mechanism for the formation of methylation products of PAHs. Along with the evolution of confined organic species in the whole MTH process, SMS initially acts as the dominant methylation agent to react with alkenes, cycloalkenes, cyclodienes, and benzene to accelerate the growth of hydrocarbon species. As the reaction progresses, the role of SMS gradually weakens, and methanol becomes the prevailing methylation agent, reacting with active HCP species during the highly efficient period and with PAHs in the deactivation stage.

Additionally, methanol and SMS, as hydride acceptors, also devote themselves to hydride-transfer reactions that lead to the formation of highly unsaturated hydrocarbon species such as dienes, active cyclic species, and PAHs. Herein, the generation of representative precursors for active HCP species (cyclopentadiene, benzene, and naphthalene) and coke species (phenanthrene, anthracene, and pyrene) was investigated to elucidate the roles of methanol and SMS in hydride-transfer reactions. As shown in Fig. 2(b), the free energy barriers for SMS-involved hydride-transfer reactions to produce cyclopentadiene (125.9–130.5 *vs.* 132.8–146.3 kJ/mol), benzene (108.1–129.1 *vs.* 127.9–144.1 kJ/mol), and naphthalene (138.3–149.5 *vs.* 139.9-150.9 kJ/mol) were lower than those for MeOH-involved reaction pathways. This suggests that SMS is relatively more effective than methanol in hydride-transfer reactions for the formation of precursors of active HCP species. On the contrary, during the deactivation stage, MeOH-involved hydride-transfer reactions for the formation of phenanthrene (148.4–151.3 *vs.* 155.7-188.4 kJ/mol), anthracene (157.2–186.7 *vs.* 167.0–195.0 kJ/mol), and pyrene (179.9 *vs.* 192.8 kJ/mol) prevail over SMS-involved reaction pathways. In terms of the SMS/methanol-involved prevailing reaction pathways, the contributions of SMS and methanol in hydride-transfer reactions are consistent with their respective roles as methylation agents at different reaction periods, further demonstrating the predominant roles of C1 reactant and intermediate (methanol and SMS) in distinct MTH reaction periods. All in all, the roles of C1 species throughout the entire MTH reaction process can be summarized as follows: during the initial stage, SMS works as the preferential C1 surface intermediate, participating in methylation reactions with alkenes, cycloalkenes, cyclodienes, and benzene to promote C–C bond formation, as well as taking part in hydride-transfer reactions to generate precursors for active HCP species. As the reaction progresses to the highly efficient and deactivation stages, methanol becomes the dominant C1 species, methylating active HCP species for efficient product formation and accepting hydrides from PAHs to cause catalyst deactivation.

3.3. Effect of the confined zeolite microenvironment with large retained organic species on methanol adsorption and SMS formation

Based on the above experimental and theoretical calculation results, C1 species (methanol and SMS) play crucial roles throughout the entire MTH process via methylation and hydride-transfer reactions. Nevertheless, the contributions of these two C1 species exhibit variability across different reaction periods. Notably, as reaction progresses to the highly efficient and deactivation stages, the role of SMS gradually weakens, which can be attributed to the influence of the confined zeolite microenvironment modified by large retained organic species. The large retained organic species generated during the continuous flow conversion of methanol are trapped in zeolite cavities and situated near BAS instead of diffusing out through the narrow pore openings [3], which modulates the zeolite microenvironment and will affect the adsorption of C1 reactants and the formation of SMS. Therefore, the influence of the confined zeolite microenvironment with large retained organic species on methanol adsorption and SMS formation was further investigated.

As shown in Fig. 3(a), methanol is initially adsorbed on BAS and then dehydrates to form SMS in the empty zeolite cavity. In contrast, when large organic species (such as PMCP, DMN, phenanthrene, pyrene, etc.) are confined in zeolite microenvironment, they occupy both acid sites and zeolite cavities, affecting the adsorption of methanol and transition states of SMS formation. The Gibbs free energy profile for SMS formation from methanol dehydration without/with large confined organic species is provided in Fig. 3(b), and the adsorption free energies of methanol and apparent free energy barriers for SMS formation are detailed in Fig. S6(a). In the empty cavity, the adsorption free energy of methanol was 15.9 kJ/mol, and the apparent free energy barrier for SMS formation was 165.2 kJ/mol. With large organic species trapped in the zeolite microenvironment, the adsorption free energies of methanol gradually increased from –1.2 kJ/mol (near PMCP) to 27.2 kJ/mol (near pyrene), and the apparent free energy barriers for SMS formation gradually increased from 159.0 to 205.5 kJ/mol. In addition, the apparent free energy barriers for SMS formation from DME (Fig. S6(b)) under the confined microenvironment were consistent with that from methanol. This illustrates that methanol adsorption and SMS formation (from methanol or DME) are affected by the confined zeolite microenvironment with the accommodation of large organic species compared to the empty cavity. It can be attributed to the interaction between large confined organics and the reactant adsorption/transition state in the CHA cavity, as evidenced by the analysis of optimized structures (Fig. 3(c) and Fig. S7). When the generated PMCP species was confined in the cavity environment, it stabilized methanol adsorption (–1.2 kJ/mol) through noncovalent interaction between the conjugated C=C bond and the hydroxyl group of methanol (the distance between the C and H atoms is about 2.3 Å). However, it also occupied the zeolite cavity and constrained the transition state, resulting in a significantly increased apparent free energy barrier (205.5 kJ/mol) for SMS formation. With the formation of PAHs, especially pyrene, it is difficult to adsorb methanol with high adsorption free energy of 27.2 kJ/mol. This suggests that an extremely weak adsorption of methanol on the acid site occurs at the later period of reaction, leading to the difficult formation of SMS in practical MTH reaction process. Therefore, at the later period of reaction, with the growth of polyaromatics confined in the zeolite microenvironment, the adsorption of methanol becomes difficult, as can be demonstrated by the increase of methanol adsorption free energies. In comparison to the empty cavity, the formation of SMS needs to overcome relatively high apparent free energy barriers with large organic species confined in the zeolite microenvironment. Both methanol adsorption and SMS formation are responsible for the observation of the absence of SMS at the later period of reaction in the *operando* spectroscopy shown in Fig. 1, and eventually, methanol dominates methylation and hydride-transfer reaction pathways to continuously drive the MTH reaction

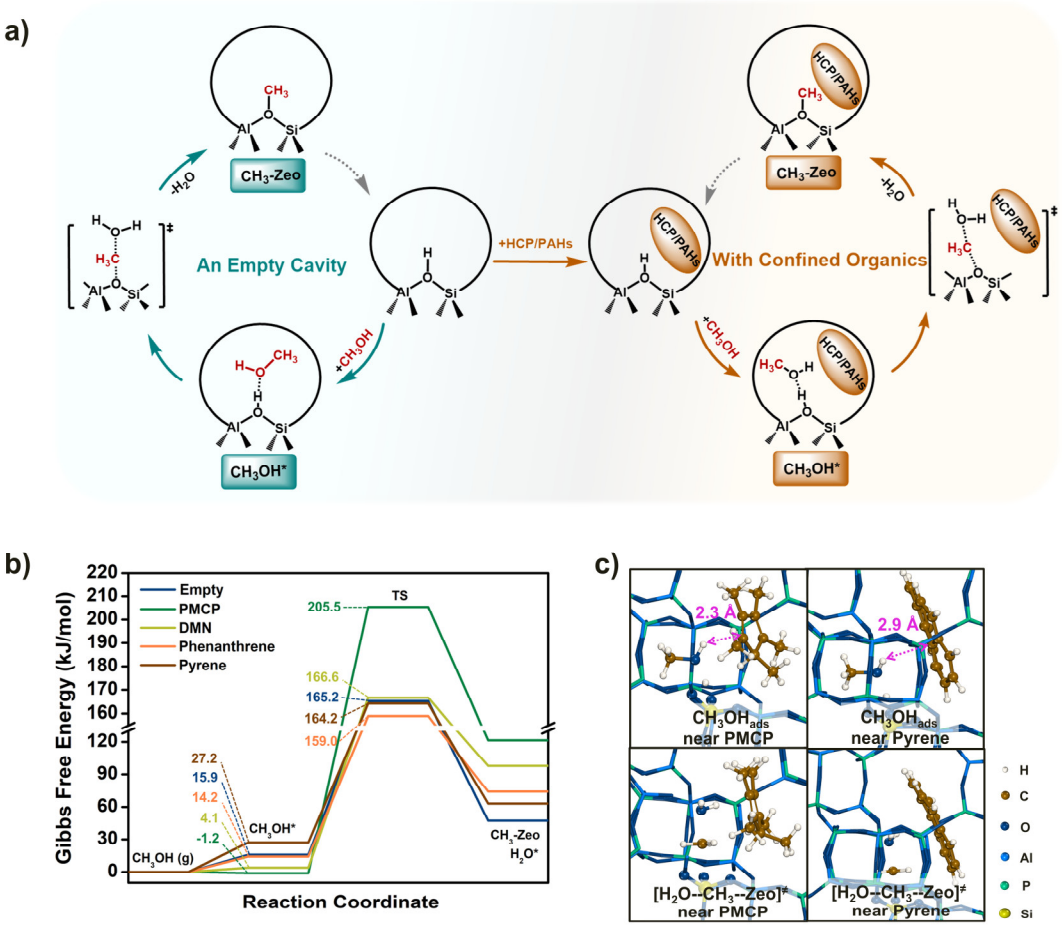

Fig. 3. (a) The schematic diagram of methanol adsorption and SMS formation in an empty cavity or with large confined organic species. (b) Gibbs free energy profile for SMS formation from methanol dehydration without/with large confined organic species at 673 K. (c) Optimized structures for methanol adsorption and transition states of SMS formation with confined PMCP or pyrene species in zeolite microenvironment.

process.

4. Conclusions

In summary, we revealed the roles of C1 species in the whole MTH reaction process by the aid of theoretical calculations and *operando* spectroscopy. The crucial C1 species, methanol and SMS, play significant roles in the MTH reaction process through participating in methylation and hydride-transfer reactions, contributing to the dynamic evolution of methanol conversion. However, the contributions of these two C1 species vary across different reaction periods. During the initial stage of reaction, SMS serves as the first and dominant C1 surface intermediate, participating in methylation reactions with alkenes, cycloalkenes, cyclodienes, and benzene to propagate C–C bonds, as well as in hydride-transfer reactions to produce highly unsaturated precursors for active HCP species. With the reaction proceeding, the role of SMS gradually diminishes, and methanol becomes the predominant C1 species, engaging in methylation reactions with active HCP species to achieve efficient product formation and accepting hydrides from PAHs to cause catalyst deactivation. Furthermore, in the later reaction period, it is highlighted that methanol adsorption and SMS formation are affected by the complex confined zeolite microenvironment, where large organic species occupy acid sites and zeolite cavities. Consequently, methanol dominates C1 species-involved reaction pathways, continuously driving the MTH reaction process. These findings support the roles of C1 species in driving the dynamic process of MTH, which goes beyond mere reactant participation, enriching the C1 chemistry.

Author contributions

Y.Z. and W.Z. conceived the study, coordinated the research, and designed the theoretical calculations and experiments. C.Z and S.L. helped in designing the experiments. L.H. and S.X. performed the NMR measurements. Y.Z., W.Z., Y.W. contributed to writing and revising the manuscript. Y.W. and Z.L. supervised the scientific work and led the collaborative efforts. All authors discussed the results and commented on the manuscript.

Electronic supporting information

Supporting information is available in the online version of this article.

Declaration of competing interest

Graphical Abstract

Chin. J. Catal., 2025, 71: 169–178 doi: 10.1016/S1872-2067(24)60228-7

The role of C1 species in the methanol-to-hydrocarbons reaction: Beyond merely being reactants

Yanan Zhang, Wenna Zhang *, Chengwei Zhang, Linhai He, Shanfan Lin, Shutao Xu, Yingxu Wei *, Zhongmin Liu
Dalian Institute of Chemical Physics, Chinese Academy of Sciences; University of Chinese Academy of Sciences

Methanol and surface methoxy species (SMS) as C1 species play crucial roles in methanol-to-hydrocarbons (MTH) process by serving as methylation agents and hydride acceptors. With reaction proceeding, the role of SMS gradually diminishes, and thereby methanol dominates reaction pathways continuously driving the dynamic evolution of MTH reaction. The contributions of these C1 species varying across different reaction periods reveal a comprehensive and systematic understanding of the roles of C1 species throughout entire MTH process, beyond the role as reactants.

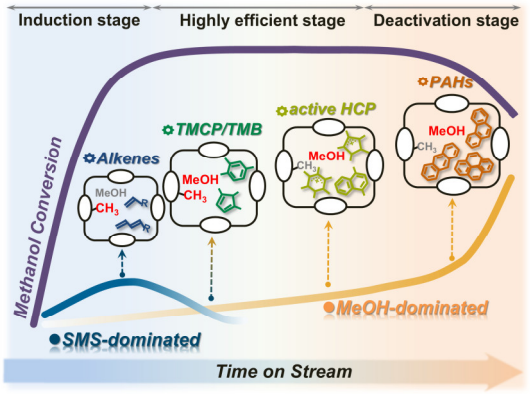

The authors declare no competing interests.

References

[1] C. D. Chang, A. J. Silvestri, *J. Catal.*, **1977**, 47, 249–259.
[2] S. Lin, Y. Zhi, W. Chen, H. Li, W. Zhang, C. Lou, X. Wu, S. Zeng, S. Xu, J. Xiao, A. Zheng, Y. Wei, Z. Liu, *J. Am. Chem. Soc.*, **2021**, 143, 12038–12052.
[3] W. Zhang, S. Lin, Y. Wei, P. Tian, M. Ye, Z. Liu, *Natl. Sci. Rev.*, **2023**, 10, nwad120.
[4] X. Wu, S. Xu, Y. Wei, W. Zhang, J. Huang, S. Xu, Y. He, S. Lin, T. Sun, Z. Liu, *ACS Catal.*, **2018**, 8, 7356–7361.
[5] X. Wu, Y. Wei, Z. Liu, *Acc. Chem. Res.*, **2023**, 56, 2001–2014.
[6] S. Lin, Y. Zhi, W. Zhang, X. Yuan, C. Zhang, M. Ye, S. Xu, Y. Wei, Z. Liu, *Chin. J. Catal.*, **2023**, 46, 11–27.
[7] S. Ilias, A. Bhan, *ACS Catal.*, **2012**, 3, 18–31.
[8] J. S. Martínez-Espín, K. De Wispelaere, T. V. W. Janssens, S. Svelle, K. P. Lillerud, P. Beato, V. Van Speybroeck, U. Olsbye, *ACS Catal.*, **2017**, 7, 5773–5780.
[9] R. Y. Brogaard, R. Henry, Y. Schuurman, A. J. Medford, P. G. Moses, P. Beato, S. Svelle, J. K. Nørskov, U. Olsbye, *J. Catal.*, **2014**, 314, 159–169.
[10] M. DeLuca, P. Kravchenko, A. Hoffman, D. Hibbitts, *ACS Catal.*, **2019**, 9, 6444–6460.
[11] H. Montalvo-Castro, M. DeLuca, L. Kilburn, D. Hibbitts, *ACS Catal.*, **2022**, 13, 99–112.
[12] S. Wang, Y. Chen, Z. Wei, Z. Qin, T. Liang, M. Dong, J. Li, W. Fan, J. Wang, *J. Phys. Chem. C.* **2016**, 120, 27964–27979.
[13] J. Chen, J. Li, Y. Wei, C. Yuan, B. Li, S. Xu, Y. Zhou, J. Wang, M. Zhang, Z. Liu, *Catal. Commun.*, **2014**, 46, 36–40.
[14] M. Svensson, S. P. Humbel, R. D. J. Froese, T. Matsubara, S. Sieber, K. Morokuma, *J. Phys. Chem.*, **1996**, 100, 19357–19363.
[15] G. W. T. M. J. Frisch, H. B. Schlegel, G. E. Scuseria, M. A. Robb, J. R. Cheeseman, G. Scalmani, V. Barone, B. Mennucci, G. A. Peters- son, H. Nakatsuji, M. Caricato, X. Li, H. P. Hratchian, A. F. Izmaylov, J. Bloino, G. Zheng, J. L. Sonnenberg, M. Hada, M. Ehara, K. Toyota, R. Fukuda, J. Hasegawa, M. Ishida, T. Nakajima, Y. Honda, O. Kitao, H. Naka, T. Vreven, J. A. ontgomery, J. E. Peralta, F. Ogliaro, M. Bearpark, J. J. Heyd, E. Brothers, K. N. Kudin, V. N. Staroverov, R. Kobayashi, J. Normand, K. Raghavachari, A. Rendell, C. J. Burant, S. S. Iyengar, J. Tomasi, M. Cossi, N. Rega, J. M. Millam, M. Klene, J. E. Knox, J. B. Cross, V. Bakken, C. Adamo, J. Jaramillo, R. Gomperts, R. E. Stratmann, O. Yazyev, A. J. Austin, R. Cammi, C. Pomelli, J. W. Ochterski, R. L. Martin, K. Morokuma, V. G. Zakrzewski, G. A. Voth, P. Salvador, J. J. Dannenberg, S. Dapprich, A. D. Daniels, O. Farkas, J. B. Foresman, J. V.Ortiz, J. Cioslowski, D. J. Fox, *Gaussian 09, revision B.01; Gaussian, Inc.: Wallingford, CT.*, **2010**.
[16] S. A. Zubkov, L. M. Kustov, V. B. Kazansky, I. Girnus, R. Fricke, *J. Chem. Soc. Faraday Trans.*, **1991**, 87, 897–900.
[17] T. R. Forester, R. F. Howe, *J. Am. Chem. Soc.*, **1987**, 109, 5076–5082.
[18] S. M. Campbell, X.-Z. Jiang, R. F. Howe, *Microporous Mesoporous Mater.*, **1999**, 29, 91–108.
[19] Q. Qian, C. Vogt, M. Mokhtar, A. M. Asiri, S. A. Al-Thabaiti, S. N. Basahel, J. Ruiz-Martínez, B. M. Weckhuysen, *ChemCatChem.* **2014**, 6, 3396–3408.
[20] L. Palumbo, F. Bonino, P. Beato, M. Bjørgen, A. Zecchina, S. Bordiga, *J. Phys. Chem. C,* **2008**, 112, 9710–9716.
[21] I. B. Minova, S. K. Matam, A. Greenaway, C. R. A. Catlow, M. D. Frogley, G. Cinque, P. A. Wright, R. F. Howe, *ACS Catal.*, **2019**, 9, 6564–6570.
[22] W. Wang, Y. Jiang, M. Hunger, *Catal. Today,* **2006**, 113, 102–114.
[23] S. Xu, A. Zheng, Y. Wei, J. Chen, J. Li, Y. Chu, M. Zhang, Q. Wang, Y. Zhou, J. Wang, F. Deng, Z. Liu, *Angew. Chem. Int. Ed.*, **2013**, 52, 11564–11568.
[24] J. Li, Y. Wei, J. Chen, P. Tian, X. Su, S. Xu, Y. Qi, Q. Wang, Y. Zhou, Y. He, Z. Liu, *J. Am. Chem. Soc.*, **2011**, 134, 836–839.
[25] I. I. Ivanova, A. Corma, *J. Phys. Chem. B*, **1997**, 101, 547–551.
[26] W. Wang, M. Seiler, M. Hunger, *J. Phys. Chem. B,* **2001**, 105, 12553–12558.
[27] Z. Wei, Y.-Y. Chen, J. Li, P. Wang, B. Jing, Y. He, M. Dong, H. Jiao, Z. Qin, J. Wang, W. Fan, *Catal. Sci. Technol.*, **2016**, 6, 5526.
[28] A. Hwang, A. Bhan, *Acc. Chem. Res.*, **2019**, 52, 2647–2656.
[29] J. Van der Mynsbrugge, S. L. C. Moors, K. De Wispelaere, V. Van Speybroeck, *ChemCatChem.*, **2014**, 6, 1906–1918.
[30] A. J. Hoffman, J. S. Bates, J. R. Di Iorio, S. V. Nystrom, C. T. Nimlos, R. Gounder, D. Hibbitts, *Angew. Chem. Int. Ed.*, **2020**, 59, 18686–18694.

[31] J. R. Di Iorio, A. J. Hoffman, C. T. Nimlos, S. Nystrom, D. Hibbitts, R. Gounder, *J. Catal.*, **2019**, 380, 161–177.
[32] A. M. Vos, K. H. L. Nulens, F. D. Proft, R. A. Schoonheydt, P. Geerlings, *J. Phys. Chem. B,* **2002**, 106, 2026–2034.
[33] S. Svelle, S. Kolboe, U. Olsbye, O. Swang, *J. Phys. Chem. B,* **2003**, 107, 5251–5260.
[34] S. Svelle, M. Visur, U. Olsbye, Saepurahman, M. Bjørgen, *Top. Catal.*, **2011**, 54, 897–906.

C1物种在甲醇制烃类反应过程中的作用：超越反应物角色

张亚楠[a,c], 张雯娜[a,*], 张成伟[a,c], 何林海[a,c], 林杉帆[a], 徐舒涛[a], 魏迎旭[a,*], 刘中民[a,b,c]
[a]中国科学院大连化学物理研究所, 低碳催化技术国家工程研究中心, 洁净能源国家实验室, 能源材料化学协同创新中心, 辽宁大连116023
[b]中国科学院大连化学物理研究所, 催化基础国家重点实验室, 辽宁大连116023
[c]中国科学院大学, 北京100049

摘要: 作为非石油资源生产包括低碳烯烃、芳烃、汽油等烃类物质的工业化路线, 甲醇制烃类(MTH)反应受到学术界和工业界的广泛关注. 在MTH反应过程中, C1物种, 包括甲醇、二甲醚和表面甲氧基物种, 在反应有机物种的演变和复杂反应网络的构建中起着至关重要的作用. C1物种不仅作为反应物, 而且还与活性烃池物种协同作用, 为自催化过程提供“燃料”并主导自催化动态演变. 然而, 在MTH复杂反应体系中, 甲醇、二甲醚、甲氧基等多种C1物种与活性烃池物种和非活性稠环芳烃物种相互作用机制以及随着反应过程的演变规律尚不明确. 因此, 深入理解C1物种在整个MTH反应过程中的重要作用是必要且具挑战的.

本文借助理论计算及谱学实验深入探究了C1物种在整个MTH复杂反应过程中的动态作用, 不仅仅是作为C1反应物的作用. 首先, 开展了原位漫反射傅立叶变换红外光谱和外原位^{13}C交叉极化魔角旋转核磁共振等谱学实验, 分析了真实MTH反应过程中反应有机物种的动态演变和多种C1物种的独特变化. 值得注意的是, 不同C1物种信号(尤其是甲醇和甲氧基)的演化随MTH反应进行存在差异, 这表明其与不同反应阶段存留有机物种的相互作用有所不同. 进一步借助密度泛函理论计算详细地揭示了甲醇和甲氧基这两种关键的C1物种, 作为甲基化试剂参与甲基化反应以及作为氢受体促进不饱和物种生成反应中的作用, 阐述了它们在MTH不同反应阶段的具体贡献差异. 在反应初始阶段, 甲氧基作为主导的C1表面物种, 与烃类物种发生甲基化反应参与C–C键的生成及碳链增长, 同时也作为氢受体促进活性烃池物种形成. 随着反应进行, 甲氧基发挥的作用逐渐减弱, 甲醇取而代之成为优势的C1物种, 参与高效期甲基化反应以生成低碳烯烃产物, 同时参与氢转移反应进一步导致催化剂积碳失活. 此外, 研究表明反应后期大体积有机物种修饰的分子筛限域微环境会影响甲醇吸附和甲氧基生成, 进一步解释了反应后期甲氧基消失的原因.

综上, 本工作对C1物种(尤其是甲醇和甲氧基)在整个MTH反应过程中的动态作用提供了全面且系统的理解, 其超越了仅仅作为C1反应物的作用, 对于丰富C1化学理论具有重要意义.

关键词: 甲醇制烃类; C1物种; 甲基化; 氢转移; 分子筛限域微环境; SAPO-34

收稿日期: 2024-11-05. 接受日期: 2024-12-18. 上网时间: 2025-04-20.
*通讯联系人. 电子信箱: zhangwn@dicp.ac.cn (张雯娜), weiyx@dicp.ac.cn (魏迎旭).
基金来源: 国家重点研发计划(2021YFA1502600); 国家自然科学基金(22372169, 22002157, 22402190, 21991092, 21991090, 22288101); 辽宁省自然科学基金(2022-BS-019).